

# Enhanced Scheme for Allocation of Primary Frequency Control Reserve Based on Grid Characteristics

Mohamad Amin Ghasemi<sup>1\*</sup>, Adel Mohseni<sup>2</sup>, Mostafa Parniani<sup>3</sup>

1- Electrical Engineering Department, University of Bu-Ali Sina, Hamedan, Iran, Email: Ma.ghasemi@basu.ac.ir

2- Iran Grid Management Company (IGMC), Tehran, Iran, Email: Mohseni@igmc.ir

3- Faculty of Electrical Engineering, Sharif University of Technology, Tehran, Iran, Email: Parniani@sharif.ir

\*Corresponding author

Received: 2020-05-23

Revised: 2020-10-09

Accepted: 2021-01-11

**Abstract**— Balancing between demand and supply of grids is the most important task of the power systems operators and control systems. Otherwise, the possibility of frequency instability and severe damages to equipment are present. Primary frequency control (PFC) is the first and main control action in the grid in front of the active power imbalance disturbances. In this paper, the effects of the spinning reserve characteristics and the grid dynamic parameters, on PFC performance and maximum frequency decline (frequency nadir), are investigated. Then, a comprehensive equation is presented to determine the maximum frequency deviation after a large power imbalance in the grid. This equation considers all effective factors such as volume and speed of the primary frequency reserve (PFR), grid inertia constant, grid load level, and the frequency-dependent loads. The correctness of the presented equation is verified through different simulations. Finally, a comprehensive scheme is proposed for the primary frequency control reserve allocation in the grid, in the form of a few equations and instructions.

**Keywords:** Primary Frequency Reserve, Inertia Constant, Load Damping Constant, Maximum Frequency Drop, Generation Ramp Rate

## 1. Introduction

Preserving the stability and security of the power grid against disturbances, and supporting the power quality requirements are the most crucial principles in the control, operation, and planning of the power system. The power system stability concept can be categorized into angular stability, voltage stability, and frequency stability, which are not independent [1]. One of the most critical factors for safe operation of the grid is to maintain frequency stability with the lowest cost. In the occurrence of a significant power imbalance between demand and supply, the system frequency will change dramatically, and the grid might collapse [2]. Therefore, precise controls and protections are designed to maintain the active power balance and the grid frequency near the nominal value.

A large active power imbalance disturbance is usually because of the sudden trip of generation units, large loads, and high load transmission lines. Nowadays, the high penetration of renewable energy resources with variable output power can also create a massive power imbalance [3]. PFC is the first, fastest, and most important control action to support the N-k security criterion and prevent unallowable frequency variation in the grid, following rapid and massive active power imbalance [4]. If the primary control could not prevent severe frequency drops, the under-frequency load shedding (UFLS) is considered as the last and most expensive control response, which, by shedding off some loads, helps to recover the frequency. Therefore, maintaining the grid frequency within the permitted range without load shedding is the main task of

PFC. Secondary and tertiary frequency controls are auxiliary controls that enter into action after the PFC function, to reduce the frequency deviation and restore the power exchange between regions to predefined values [5]. The base and backbone of PFC is the Primary Frequency Reserve (PFR) which its specifications have significant effects on its performance. The grid frequency control has been a matter of concern for researchers for some decays, and various papers have discussed on amount of reserve for primary and secondary frequency control, especially in the presence of high penetration of renewable energy resources. Accordingly, different deterministic and probabilistic methods have been presented to allocate PFR [3, 4, 6-13]. However, less attention has been paid to the detailed requirement of the PFR. Also, the effective parameters such as ramp rate limit of units, the load level of the grid, and the reserve allocation scheme between units have not been gotten enough attention [12]. Because of the high-speed operation of PFC, in comparison with secondary and tertiary control, it should be provided by high-speed generation units (high ramp rate). Evaluating the ramp rate of different power plants has received increasing attention for grid operators, and various industrial projects have been defined for assessing the response time of the power plants in front of a step and ramp change in grid frequency [14, 15]. Accordingly, the capability and accurate dynamic models of different power plants extracted, and better PFC reserve allocation can be done. Furthermore, with the advent of micro-grids, renewable energy sources, controllable loads, and smart grids, the topic of PFC in advanced grids are getting

attention increasingly [16]. The possibility of providing PFR using controllable loads and renewable energy resources such as wind turbines and solar power plants has been the subject of various articles [17].

On the other hand, to encourage the power plants to participate in PFC and providing PFR, various markets and pricing schemes have been proposed and used worldwide in which the price is mostly based on reserve MW volume [18]. However, the speed of reserve and the ramp rate of power plants also should be considered in the pricing of the PFR. Anyway, providing a method for allocating the minimum reserve MW capacity results in significant cost reduction.

Above all, since both PFC and UFLS are responsible for ensuring the grid frequency stability, their design should be coordinated. However, less attention has been paid to these important issues so far [12]. The most important parameter in coordinating PFC and UFLS is maximum frequency drop after disturbance (frequency nadir), which is a significant indicator for grid frequency security. Indeed, PFC must stop frequency drop before reaching the UFLS thresholds. Therefore, estimation of the frequency nadir and determining the effective parameters, could be very useful in PFR allocation. In the previous studies, some methods have been proposed to estimate frequency nadir after disturbance in power system [19-23] which most of them are based on the system frequency response (SFR) model. Reference [19] analyzed the effect of the dead band in PFC loop on frequency nadir. It has improved the method of [20], but it is so complicated and similar to [20], has not considered the ramp rate of units [12]. This parameter is not also considered in the presented method in [21]. The proposed method in [22] uses machine learning and clustering the probable scenarios in the grid to predict the frequency nadir. Also, reference [23] uses ANN to predict the frequency nadir value. This method is complicated and time-consuming, which can decrease its applicability in real power systems. Accordingly, as the contributions of this paper, the effective parameters on the dynamic frequency response of the grid are discussed in detail. Then, considering all effective parameters, a simple and comprehensive equation is proposed to estimate the frequency nadir. Finally, using the aforementioned equation and considering the interaction of PFC with UFLS, an enhanced method for allocating the primary frequency reserve is proposed. The proposed method gives a comprehensive information about the effective parameters on PFC performance in the form of a few simple equations, which can be very useful for the grid operators. Since it considers all effective parameters, it is not needed to allocate conservative PFR. Indeed, with a minimum volume of reserve and allocating the determined reserve properly between the candidate unit, the cost of PFR is reduced.

The rest of the paper is organized as follows. In Section 2, the modeling of the power system for frequency studies presented. The general frequency control strategy of power systems is explained briefly in Section 3, with an emphasis on primary frequency control and active power reserves. In Section 4, the effect of different parameters on the frequency behavior of the system is studied. A comprehensive equation is presented in section 5 to determine the maximum frequency deviation of the grid after a power imbalance disturbance. According to the results of previous sections, a new plan for allocation of

the PFR, coordinated with power system security and UFLS scheme, is presented in section 6. The conclusion is the last part of the paper.

## 2. Modeling of power system for frequency studies

The issue of frequency stability studies and the design of proper control strategy requires an appropriate model of the power system and its effective parts. In this regard, detailed modeling of all parts is not necessary, and only those parts, equipment, and controllers, which their function is in the time range of PFC and UFLS operation, are intended. The related parts include the frequency dependency of loads, turbine-governor of power plants, and somewhat the transmission system.

Although there is some oscillatory difference between the frequency of busbars in the grid, after power imbalance disturbance [24], considering the preserved angular stability of the power system, the average value of frequency in all buses is equal; therefore, the transmission system can be ignored in frequency studies. Accordingly, one can use a single bus grid model where all loads and power plant units are connected to one hypothetical busbar. However, the effect of the transmission system on the angular and voltage stability is very important.

Generally, the frequency behavior of power plants can be presented by the swing equation. This equation shows the relation between the frequency deviation ( $\Delta\omega$ ) of generated voltage with the change of its input mechanical power  $\Delta P_m$ , and output electrical power ( $\Delta P_L$ ) as follows [25]:

$$2H \frac{d\Delta\omega}{dt} = \Delta P_m - \Delta P_L \quad (1)$$

in which,  $H$  is the inertia constant of rotor-turbine combination. Also, for more types of loads in the grid, the active power consumption changes with the grid frequency changes. This dependency is modeled as

$$\Delta P_L = \Delta P_{L0} + D\Delta\omega \quad (2)$$

That  $D = \partial PL / \partial\omega$  is known as the load damping constant, and  $\Delta P_{L0}$  is the frequency-independent part of the load. Combining the swing equation of all ( $N$ ) power plants with the frequency-dependent model of all ( $K$ ) loads results in

$$\begin{aligned} 2H_1 \frac{d\Delta\omega_{pu}}{dt} + \dots + 2H_N \frac{d\Delta\omega_{pu}}{dt} \\ = \Delta P_{m-1} + \dots + \Delta P_{m-N} - \Delta P_{L0-1} - D_1 \Delta\omega_{pu} \\ - \dots - P_{L0-K} - D_K \Delta\omega_{pu} \end{aligned} \quad (3)$$

$$2 \left( \sum_{i=1}^N H_i \right) \frac{d\Delta\omega_{pu}}{dt} = \sum_{i=1}^N P_{m-i} - \sum_{j=1}^K \Delta P_{L0-j} - \sum_{j=1}^K D_j \Delta\omega_{pu}$$

Considering  $(\sum_{i=1}^N H_i)$  as equivalent inertia constant ( $H_{eq}$ ) of the grid and  $\sum_{j=1}^K D_j$  as equivalent load damping constant of the grid ( $D_{eq}$ ), and transferring (3) to Laplace form yields the following equation between grid frequency variations ( $\Delta f_{pu}$ ) and power imbalance between total generation ( $\sum \Delta P_{m-i}(s)$ ) and total consumption ( $\sum \Delta P_{L0-j}(s)$ ).

$$\begin{aligned} \Delta\omega_{pu}(s) &= \Delta f_{pu}(s) \\ &= \frac{\sum \Delta P_{m-i}(s) - \sum \Delta P_{L0-j}(s)}{2H_{eq} s + D_{eq}} \end{aligned} \quad (4)$$

In power plant units, the governor is a system used to control and adjust the turbine mechanical power ( $P_m$ ). Fig.

1 shows a simple and general model of a turbine-governor system. Inputs of the governor are generally the feedback value of  $P_m$ , the unit dispatched power ( $P_{disp}$ ), and the grid frequency. The reference value of unit power ( $P_{ref}$ ) is equal to dispatched power ( $P_{disp}$ ) of the unit in the steady-state; However, for units participating in primary frequency control, there is a feedback in the governor which manipulates  $P_{ref}$  proportional to  $\Delta\omega$ . Indeed, the coefficient of  $1/R$  ( $R$  is called droop) operates as a proportional controller and manipulates  $P_{ref}$ . The output of the governor is the position of control valves which changes the turbine mechanical power. Ignoring the details, the turbine can be modeled with a time constant. Furthermore, there are two constraints that show the intrinsic limits of the power unit. The first constraint is a rate limiter that models the maximum speed of the turbine in increasing ( $R_{max}$ ) and decreasing ( $R_{min}$ ) its generation. It should be mentioned that the value of  $R_{min}$  and  $R_{max}$  is lower when the unit is in normal loading conditions. Indeed, their values are much more in primary control mode than in normal loading conditions. The second constraint models the maximum ( $P_{max}$ ) and minimum power ( $P_{min}$ ) that the turbine can generate. Indeed, the high-speed changes of output power can be around  $P_{dis}$  in the range of  $[P_{min} P_{max}]$ . Accordingly, the difference between  $P_{max}$  and  $P_{dis}$  is called the PFR of the unit.

It worth mentioning that the different type of turbine governors has their own particular model, but it will be shown in Sec. 5, that, in state of a significant power disturbance in the grid, all units behave similarly in PFC, and the presented model in Fig. 1 can be used for all of them.

Considering the dynamic model of (4) and the turbine governor model in Fig. 1, the system frequency response (SFR) model is constructed, as shown in Fig. 2. This model is relatively a complete model for the grid frequency analyses. In this model, it is supposed that  $n$  units are participating in PFC, which have their own limits in the amount and the speed of power changes. In the normal grid state,  $\Delta\omega$  is so small, and  $P_{ref}$  and  $P_m$  of all units are equal to their corresponding  $P_{disp}$ . Therefore, the total value of the grid load ( $P_{L0}$ ) is equal to the sum of the  $P_{disp}$ s of all units. Hence, the effect of  $P_{disp}$ s and  $P_{L0}$  are canceled and are not shown in the final model (Fig. 2). Accordingly, only load variations ( $\Delta P_L$ ) and the power variation of units, caused by PFC, are considered. The UFLS is also presented in this model.

Given the fact that lot of units are participating in the PFC of a large grid, the SFR model and its analysis will be complicated. However, the SFR model can be simplified, and the primary control loops of all units can be modeled in the one equivalent loop with equivalent parameters, as shown in Fig. 3. It should be mentioned that the equivalent SFR model in Fig. 3 is valid in all conditions, but the values of  $R_{max-eq}$ ,  $R_{min-eq}$ ,  $R_{eq}$ , and other equivalent parameters are not constant and change during the response to different values of  $\Delta P_L$  disturbance. Indeed, for some values of disturbance ( $\Delta P_L$ ), the output of some units reaches their  $P_{max}$  limit and doesn't respond to further frequency deviations. Hence, it is ignored from SFR model; thus, the equivalent parameters of  $R_{max-eq}$ ,  $R_{min-eq}$ ,  $R_{eq}$  change.

### 3. Grid frequency control

Active power control is one of the most important tasks of the operator to keep the grid frequency near the nominal value, with supporting the constraints on generation units and transmission system. In modern power systems, three hierarchical control mechanisms are used to control the generation and frequency of the grid, which are tertiary, secondary, and primary controls. Tertiary is the slowest one that determines the dispatched (reference) power of the units, based on economic and technical parameters. However, secondary and primary controls act in the occurrence of the power disturbance.

Following a large imbalance in the power system, such as a power plant trip or the disconnection of a highly loaded transmission line, three consequences occur in the following order [1]:

- 1- generator rotors oscillate, and the grid frequency starts to decline,
2. because of frequency deviation, the primary frequency control is activated to stop the frequency decline and restores it to near the nominal value (it takes from several seconds until several ten seconds),
3. the secondary control is activated as a centralized control, and by changing the  $P_{disp}$  of prespecified units or by connecting new units to the grid, restores the grid frequency and power flow of the tie lines.

It should be mentioned that in deficiency of the primary control reserve, the frequency decline continues until UFLS is activated to stop the frequency decline by shedding some of the loads.

Fig. 1 shows the overall operation of the primary and secondary control in the grid frequency recovery with emphasis on their operation time interval. It should be noted that based on the arguments presented in later sections, the operation time interval of the primary control depends on the dynamic characteristics of the grid, and is not the same for all power systems.

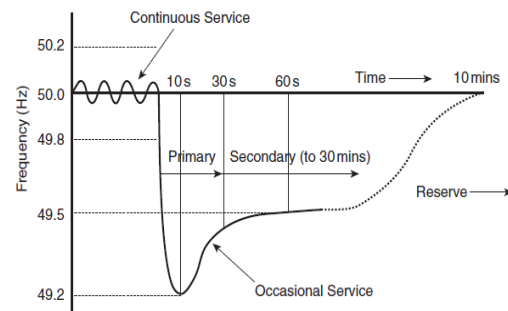


Fig. 1. Response time of primary and secondary control in a sample power system after power imbalance disturbance [7].

Active power reserve is the backbone of PFC. In definition, flexibility in the change of active power generation in the grid is called active power reserve and can be categorized into two types, including spinning and non-spinning reserves [6].

**Spinning Reserve** is the free capacity of the grid synchronized generation units, which can be released and used in lower than some minutes if needed.

**Non-Spinning reserve** is the installed generation capacity of the grid, whose units are not grid-synchronized, while they can be integrated into the grid and generate power if needed.

**Table I:** Two categorization of power reserve and their relationship

First category	Second category
Spinning Reserve	PFR
	Secondary Frequency Reserve
Non-Spinning Reserve	Tertiary Reserve

In other categorization, the active power reserve can be divided into three types, including primary, secondary, and tertiary reserve, based on their response time (the time that they can be available) [6-8]. The reserve that a generation unit can provide for the grid, depends on the dynamic characteristics of the unit including its  $R_{max}$  and  $R_{min}$ . In this regard, the high-speed reserve which is provided by high-speed units (high values of  $R_{max}$  and  $R_{min}$ ) is called PFR and used in PFC. Accordingly, the existence of this reserve is necessary and should be resealed in the first few seconds after power imbalance disturbance in the grid. Meanwhile, it must have the capability to stay available at least for a few minutes [4]. According to the turbine-governor model in Fig. 1 and the SFR model in Fig. 2, the power interval  $[P_{min} P_{max}]$ , that the unit has high speed in changing power (in the range of  $[R_{min} R_{max}]$ ), represent the PFR concept, and the difference between  $P_{disp}$  and  $P_{max}$  is the value of PFR provided by each unit. The power reserves that are slower and obtained by slower units are

used in the secondary control and considered in the secondary reserve category. The part of non-spinning reserves that can be quickly synchronized with the grid, such as small gas units, are also classified as a secondary reserve. The tertiary reserve is the non-spinning reserve, which can be synchronized to the grid based on grid load and economic dispatch. Table I shows two main categories of active power reserve in a grid and their relationship with each other. Fig. 5 also shows the characteristic of primary and secondary reserves with an emphasis on their response time. It is noted that contrary to [8],  $T_1$ ,  $T_2$ , and  $T_3$  are not constant and dependent on the load level and characteristics of the grids.

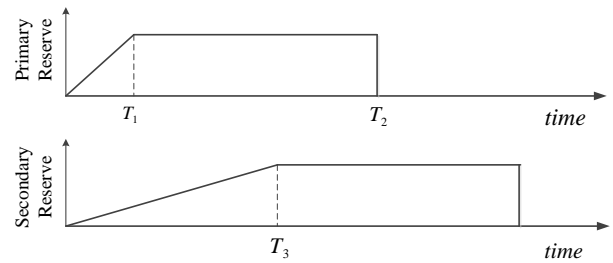


**Fig. 2.** Time-response characteristic of primary and secondary reserves.

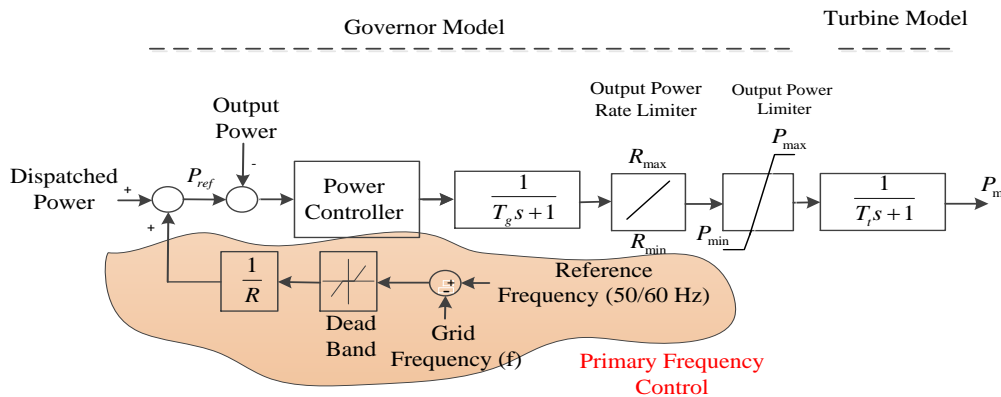


**Fig. 3.** General turbine-governor model of generation units.

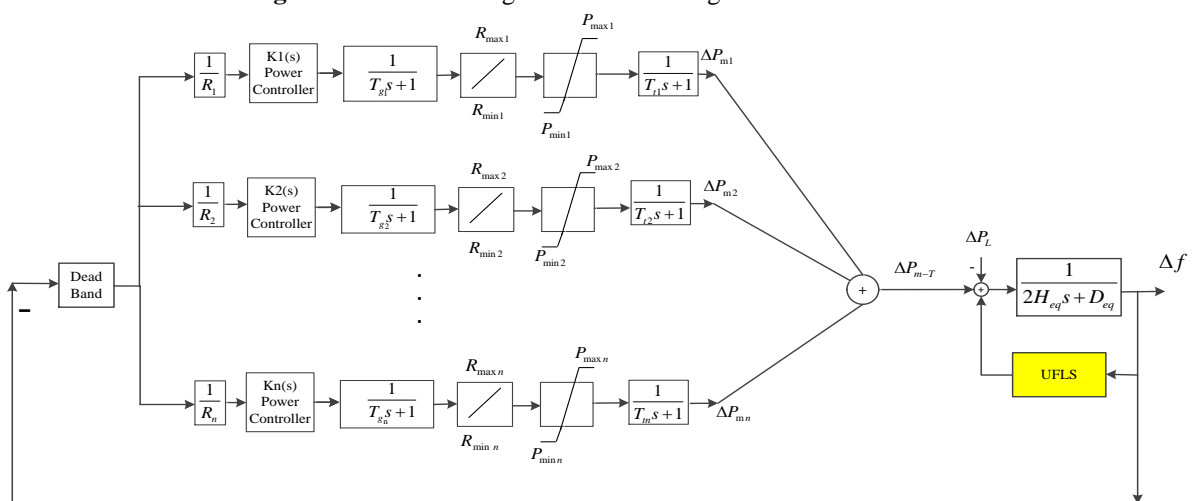


**Fig. 4.** System frequency response (SFR) model of a power grid

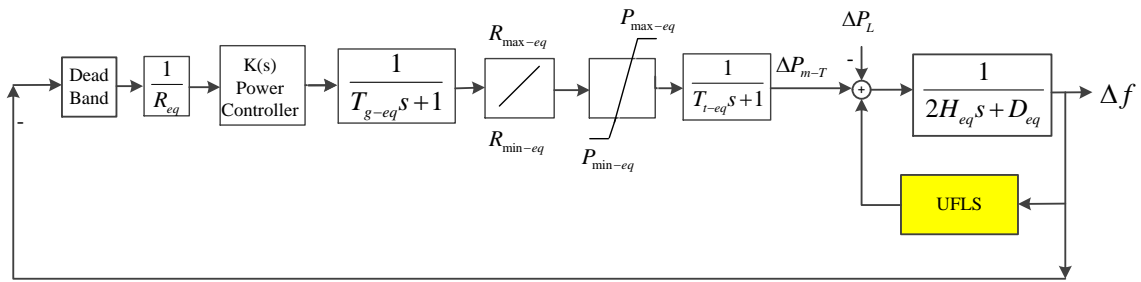


Fig. 5. Simplified equivalent SFR model of a power grid

#### 4. Effect of the grid and PFR characteristics on the grid frequency behavior

Most power systems worldwide currently allocate primary and secondary reserve based on well-known N-1 security criterion [26]. Based on Union for the Co-ordination of Transmission of Electricity (UCTE) and North American Electric Reliability Council (NERC) requirement, the total PFRs volume must be equal to the active power generation of the largest unit in the grid [10]. Summary of the primary control standards in UCTE and NERC presented in Table II.

Table II: PFR standards [10]

Standard	UTCE	NERC
Full Availability	$\leq 30\text{ s}$	$\leq 60\text{ s}$
Deployment ends	$\geq 15\text{ min}$	$\geq 10\text{ min}$

However, it can be shown that unlike what is shown in Fig. 5 and Table II, the time characteristic of the PFR is not the same for all grids and is dependent on various parameters of the grid. Furthermore, even for a specific grid, it is not constant and dependent on load level and other characteristics. This issue is discussed in the following, and, based on dynamic parameters of the grid, the desired specifications of a PFR are presented.

It is noted that the final frequency deviation ( $\Delta f(\infty)$ ) after power imbalance disturbance, the frequency nadir ( $f_{min}$ ), and the occurrence time of  $f_{min}$  ( $t_{min}$ ) are as the most important characteristics in the frequency behavior of the system. In the following, it is tried to investigate the effects of power system parameters, such as the  $H_{eq}$ ,  $R_{eq}$ ,  $D_{eq}$ , total PFR ( $P_{max-eq}$ ), its allocation scheme between units, and  $R_{max-eq}$  on frequency behavior of the system. In this regard, the equivalent SFR model of the grid (in Fig. 3) is simulated in different conditions in Matlab/Simulink. The specification of the simulated system is shown in Table III. it should be noted that the value of R for the units is usually about  $0.05\text{ pu/pu}$  in a real power system, and assuming that, for example, 33% of the synchronized units participate in the PFC,  $R_{eq}$  will be about  $0.15\text{ pu/pu}$ .

As mentioned previously, the main importance of  $f_{min}$  is due to UFLS scheme in the grid. In the most worldwide grids, UFLS scheme is static, and a certain amount of grid load is shed at some certain frequency thresholds. While to establish the N-1 security criterion in the grid, the PFC and the associated reserve should be able to prevent the reach of the frequency to the first step of UFLS ( $f_{sh-1}$ ), after the trip of the largest unit. As well, the importance of  $t_{min}$  is

that, before  $t_{min}$ , the sufficient PFR must be deployed into the grid and prevent further frequency deviation. Indeed, for a larger value of  $t_{min}$ , the speed of PFR can be lower, and vice versa.

Since an specific power systems may have different values of  $H_{eq}$ ,  $D_{eq}$ ,  $P_{max-eq}$ , and  $R_{max-eq}$  in different load levels, to consider all possible conditions, the behavior of the system is investigated in the following scenarios.

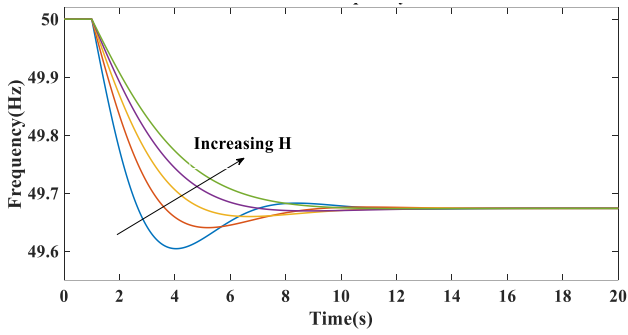
- 1) There is no limit on reserve value ( $P_{max-eq}$  and  $P_{min-eq}$ ) and its speeds ( $R_{max-eq}$  and  $R_{min-eq}$ ), and the value of  $H_{eq}$  is changed from 5s to 13s.
- 2) There is no limit on reserve value ( $P_{max-eq}$  and  $P_{min-eq}$ ) and its speeds ( $R_{max-eq}$  and  $R_{min-eq}$ ), and the value of  $D_{eq}$  is changed from 0 to  $2\text{ pu/pu}$ .
- 3) There is no limit on reserve speed ( $R_{max-eq}$  and  $R_{min-eq}$ ), but the volume of the reserve is limited.
- 4) There is no limit on the PFR value ( $P_{max-eq}$ ), but its speeds ( $R_{max-eq}$  and  $R_{min-eq}$ ) are limited.
- 5) Both the volume and speed of the reserve are limited.
- 6)  $P_{max-eq}$  is greater than the simulated power disturbance, but it is not allocated equally between the units.

Table III. Parameter values of the simulated SFR model in Fig. 3

Parameters	Value
$H_{eq}$	$\infty\text{ s}$
$D_{eq}$	$1\text{ pu/pu}$
$R_{eq}$	$0.15\text{ pu/pu}$
$T_{g-eq}$	$0.2\text{ s}$
$T_{t-eq}$	$1\text{ s}$

##### 4.1 There is no limit on the amount and speed of PFR, and $H_{eq}$ is changed from 5s to 13s.

In this test, a disturbance as  $\Delta P_L = 0.05\text{ pu}$  is applied to the system, and  $H_{eq}$  is changed from 5 to 13s. The frequency behaviors of the system are shown in Fig. 6 for different values of  $H_{eq}$ . Increasing the value of  $H_{eq}$  increases  $f_{min}$  and  $t_{min}$ . This phenomenon indicates that, for the higher value of  $H_{eq}$ , the PFC has more time to release the reserve and prevent further frequency drop. Therefore, the speed of the allocated PFR can be lower.



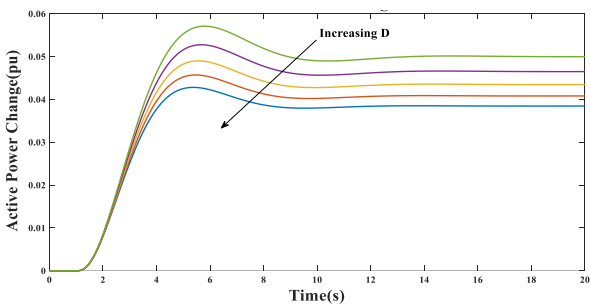
**Fig. 6.** Frequency behavior of the grid after  $\Delta P_L = 0.05$  pu for different values of  $H_{eq}$ , and without any limit on volume and speed of reserve.

4.2 There is no limit on the amount and speed of PFR, and  $D_{eq}$  is changed from 0 to  $2pu/pu$ .

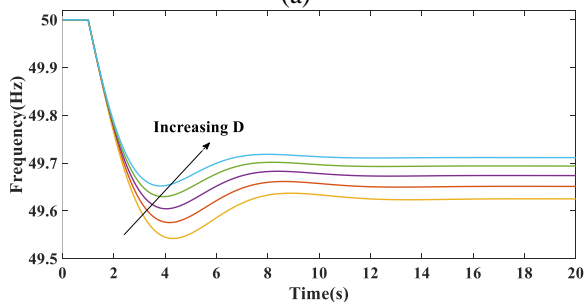
A power imbalance disturbance as  $\Delta P_L = 0.05pu$  is applied to the system. The frequency behaviors of the system and  $\Delta P_{m-T}$  are shown in Fig. 7 for different values of  $D_{eq}$ . When the value of  $D_{eq}$  increases, the  $f_{min}$  and  $f_{\infty}$  increase, and  $\Delta P_{m-T}$  decreases. Hence, for the systems with the higher values of  $D_{eq}$ , a lower amount of the PFR is needed.

4.3. Limit on the reserve amount, no limit on the speed of reserve:

In this case, the PFR amount is set to 0.04 pu, which is less than the imposed disturbance to the system ( $\Delta P_L = 0.05$  pu). Fig. 8 shows the frequency behavior, in which the  $f_{\infty}$  becomes 49.5 Hz, which is not an acceptable value. Also, the maximum frequency drop is much higher than the cases without any limit on the reserve (Fig. 6). In this case, the shortage of the reserve is compensated by the cost of more frequency drop and reduction in load due to the non-zero value of  $D_{eq}$ . According to (5), the shortage of PFR has decreased the  $R_{eq}$  of the system from  $R_{eq} = 0.15$  to  $R_{eq-new} = 0.25$ .



(a)



(b)

**Fig. 7.** Frequency behavior of the grid (a), and active power generation changes (b), after  $\Delta P_L = 0.05$  pu, for different values of  $D_{eq}$ , and without any limit on volume

and speed of the reserve.

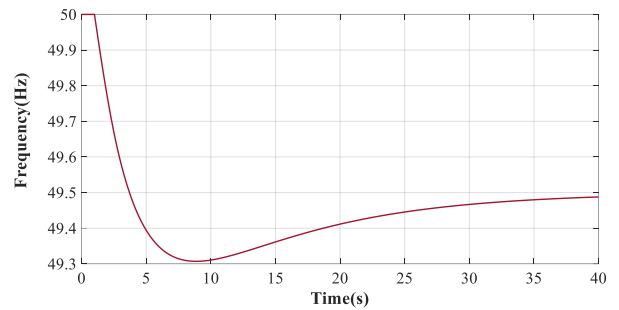


**Fig. 8.** Frequency behavior of the grid after  $\Delta P_L = 0.05$  pu, for  $P_{max-eq} = 0.04$  pu and no limit on the reserve speed.

4.4 There is no limit on the reserve amount, but its speed is limited

Regarding the limited number of participating units in PFC of a real grids,  $R_{max-eq}$  and  $R_{min-eq}$  are limited. In this simulation, the values of  $R_{max-eq}$  and  $R_{min-eq}$  are set to  $R_{max} = 0.002 pu/s$  and  $R_{min} = -0.003 pu/s$ , which are near to their practical values [23]. The frequency behaviors of the system, for 3 different values of  $H_{eq}$  and  $\Delta P_L = 0.05$  pu, are shown in Fig. 9. It is seen that, for all  $H_{eq}$ , the  $f_{min}$  is much lower than that of the case without any limit on reserve speed (Fig.6). Although there is enough PFR, if the first step of UFLS is supposed on 49.4 Hz, for  $H_{eq} = 5s$  and  $10s$ , the frequency drop will activate UFLS. Indeed, this means that the available PFR hasn't been used optimally and despite the sufficient volume of the reserve, the N-1 security criterion is not supported. However, increasing the number of participating units in PFC increases  $R_{max-eq}$  as well, and frequency behavior is improved. Besides, for a larger value of inertia (*e.g.*  $H_{eq} = 20s$ ),  $f_{min}$  is larger than  $f_{shed-1}$ , and UFLS is not activated. This means that the required speed of the PFR depends not only on  $\Delta P_L$  but also on  $H_{eq}$ .

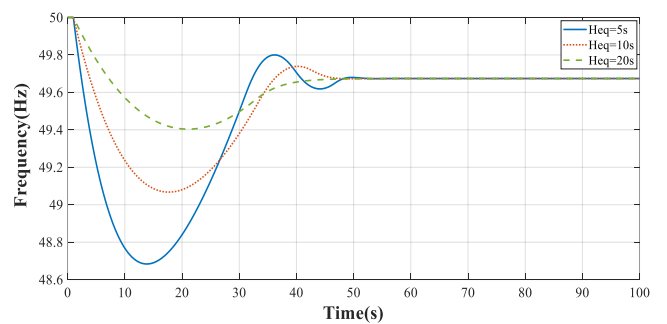


**Fig. 9.** Frequency behavior of the grid for different values of  $H_{eq}$  after  $\Delta P_L = 0.05$  pu ( $R_{max-eq} = 0.002 pu/s$  and  $R_{min-eq} = -0.003 pu/s$ , and no limit on reserve volume).

4.5. There are limits on both the volume and the speed of the PFR

In this case, the reserve value is set to  $P_{max-eq} = 0.04 pu$  and its releasing speed is set to  $R_{max-eq} = 0.002 pu/s$  and  $R_{min-eq} = -0.003 pu/s$ . The frequency behavior is shown in Fig. 10 for  $\Delta P_L = 0.05$  pu. it can be seen  $f_{\infty} = 49.5$  Hz and  $f_{min} = 48.55$  Hz, and considering the first UFLS relay on 49.4 Hz, load shedding relays will operate.

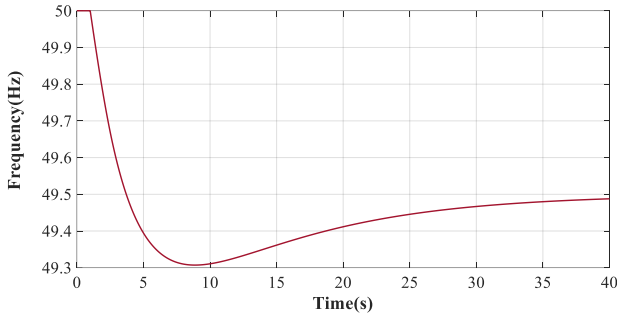


**Fig. 10.** Frequency behavior of the grid after  $\Delta P_L = 0.05$  pu ( $R_{max-eq} = 0.002$  pu/s and  $R_{min-eq} = -0.003$  pu/s, and the reserve volume of  $P_{max-eq} = 0.04$  pu).

#### 4.6. There is sufficient reserve, but not properly divided between units

In this simulation, it is assumed that there are two identical units in the PFC (SFR model of the system in Fig. 2 with two units). In the first case, the total reserve is  $P_{max-eq} = 0.05$  pu, which 0.035 pu is gotten from the first unit ( $P_{max-1} = 0.035$  pu) and 0.015 pu from the second unit ( $P_{max-2} = 0.015$  pu), and the disturbance is as  $\Delta P_L = 0.05$  pu. Accordingly, there is no shortage in PFR volume. In the second case, the PFR volume of 0.05 pu is equally divided between two units, and each unit provides 0.025 pu of reserve. In Fig. 11, the frequency response of the system in both cases are compared with each other. It can be seen from Fig. 11 that the unequal allocation of the reserve between units not only affects the  $f_{min}$ , but also decreases  $f_{\infty}$ , which means inappropriate use of the PFR.

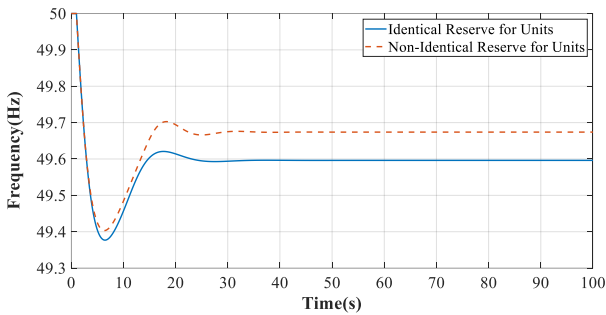


**Fig. 11.** Frequency behavior of the grid after  $\Delta P_L = 0.05$  pu, for two different reserve allocation schemes: 1- balanced between units, 2- unbalanced between units.

In summary, the results of the above simulations show that the value of  $H_{eq}$ ,  $D_{eq}$ , and speed, volume, and allocation scheme of the reserve have a significant effect on the frequency behavior of the system. In the next section, it is tried to provide mathematical relations between  $f_{min}$ ,  $H_{eq}$ ,  $D_{eq}$ , speed, and the amount of the reserve.

### 5. Maximum frequency deviation in power imbalance disturbance

As already noted, to establish N-1 security criterion in the grid, the PFC and the PFR should be able to prevent the frequency decline to  $f_{shed-1}$  after the trip of the largest unit. To do so, an analytical method is proposed to obtain the  $f_{min}$ , after power imbalance disturbance, based on the grid characteristics and PFR features. Accordingly, the characteristics of a suitable grid-based PFR are presented.

First, it is assumed that, in the PFC model of Fig. 3, there is no limit on the amount of the reserve. According to the authors' surveys, although  $R_{max}$  of units depends on the type and other characteristics of units, the average value of  $R_{max}$  for participant units in the PFC is about  $R_{max-i} = 0.005$  pu/s, based on the nominal power of the unit [23]. On the other hand, the typical droop coefficient  $R = 0.05$  pu/pu for units leads to a high gain ( $1/R = 20$ ) in the PFC loop. Accordingly, considering the high gain of the PFC loop and the low value of  $R_{max}$ , a small frequency deviation (out of dead band) in the grid activates the speed limit of units and the power change rate of units is limited to their  $R_{max}$ . Hence, the contribution of units in the PFC, after the trip of the largest unit, is the increase of active power with the maximum speed ( $R_{max}$ ). Therefore, the total equivalent active power variations in the grid can be models as:

$$\begin{aligned} \Delta P_{m-T}(t) &= \sum \Delta P_{m-i}(t) \\ &\approx \sum R_{max-i} t = R_{max-eq} t \end{aligned} \quad (5)$$

Which can be represented in the Laplace domain as

$$\Delta P_{m-T}(s) = \frac{R_{max-eq}}{s^2} \quad (6)$$

Therefore, considering the grid model in (4) and the power imbalance applied to the grid ( $\Delta P_L$ ), the dynamic response of the grid frequency, in the Laplace domain, will be as follows.

$$\Delta f(s) = \left[ \frac{R_{max-eq}}{s^2} - \frac{\Delta P_L}{s} - D_{eq} \Delta f(s) \right] \cdot \left[ \frac{1}{2H_{eq}s} \right] \quad (7)$$

As a result, the following relation is obtained

$$\Delta f(t) = \frac{-2H \cdot R_{max-eq}}{D_{eq}^2} u(t) + \frac{R_{max-eq}}{D_{eq}} tu(t) + \frac{2H \cdot R_{max-eq}}{D_{eq}^2} e^{-\frac{D_{eq}t}{2H_{eq}}} u(t) - \frac{\Delta P_L}{D_{eq}} u(t) + \frac{\Delta P_L}{D_{eq}} e^{-\frac{D_{eq}t}{2H_{eq}}} u(t) \quad (9)$$

$$t_{min} = \frac{\Delta P_L - D_{eq} \cdot \Delta f_{max}}{R_{max-eq}} \quad (10)$$

$$\Delta f_{max(pu)} = - \frac{\Delta P_{Lpu} \cdot D_{eq} + 2H_{eq} R_{max-eq} \ln \left( \frac{2H_{eq} R_{max-eq}}{2H_{eq} R_{max-eq} + \Delta P_{Lpu} \cdot D_{eq}} \right)}{D_{eq}^2} \quad (11)$$

$$\Delta f_{max(pu)} = \frac{\Delta P_L - P_{max-eq}}{D_{eq}} \quad (12)$$

$$\Delta f_{max(pu)} = \max \left( \frac{\Delta P_L - P_{max-eq}}{D_{eq}}, \left[ \frac{\Delta P_{Lpu} \cdot D_{eq} + 2H_{eq} R_{max-eq} \ln \left( \frac{2H_{eq} R_{max-eq}}{2H_{eq} R_{max-eq} + \Delta P_{Lpu} \cdot D_{eq}} \right)}{D_{eq}^2} \right] \right) \quad (13)$$

$$\Delta f(s) = \frac{1}{2H_{eq}} \cdot \left[ \frac{R_{max-eq}}{s^2 \left( s + \frac{D_{eq}}{2H_{eq}} \right)} - \frac{\Delta P_L}{s \left( s + \frac{D_{eq}}{2H_{eq}} \right)} \right] \quad (8)$$

Using inverse Laplace transformation, the frequency behavior of the system, in the time domain, will be as (9). On the other hand, the frequency decline continues as far as the active power balance is achieved again. Indeed, when the  $\Delta P_{m-T}$  becomes equal to sum of  $\Delta P_L$  and frequency-dependent load change ( $D_{eq} \Delta f$ ), the frequency decline stops. At this moment, which is called  $t_{min}$ ,  $f_{min} = f_{nom} - \Delta f_{max}$  takes place. Accordingly,  $t_{min}$  can be determined by (10). Putting  $t_{min}$  from (10) in (9),  $\Delta f_{max}$  is obtained as (11). Then, putting  $\Delta f_{max(pu)}$  from (11) in (10), the value of  $t_{min}$  is also obtained.

In the above relations, it was assumed that until  $t_{min}$ , the amount of PFR is not limited and the production of units is increasing continuously. In other words,  $\Delta P_{m-T}(t_{min}) = R_{max-eq} t_{min}$  is less than  $P_{max-eq}$ . However, if  $R_{max-eq} t_{min}$  is greater than  $P_{max-eq}$ , before reaching  $t_{min}$ , the total volume of the PFR is released, but the frequency drop is not stopped. Therefore, the frequency drop continues until the active power balance is restored due to the reduction in consumption of frequency-dependent loads. In this case, the  $f_{min}$  is obtained from the following equation.

Generally, if  $R_{max-eq} t_{min} \leq P_{max-eq}$ , then the absolute value of  $\Delta f_{max}$  in (12) is lower than that of (11). Therefore, it can be shown easily that the general relation of  $\Delta f_{max}$  is the maximum value of (11) and (12), which can be represented as (13).

The presented equation for  $\Delta f_{max}$  in (13) is valid for all situations. While the relation in (12) is valid if  $R_{max-eq} t_{min} \leq P_{max-eq}$ , and (11) is valid when  $R_{max-eq} t_{min} > P_{max-eq}$ . To verify the presented equation in (13), two examples are given in the following.

- A.** For a disturbance value of  $\Delta P_L = 0.04 pu$ , the PFR volume  $P_{max-eq} = 0.04 pu$ ,  $R_{max-eq} = 0.002 pu/s$ , and the system parameters presented in Table 3, the value of  $\Delta f_{max}$  from (13) will be as follows.

$$\Delta f_{max}(pu) = \max(0, 0.018) \triangleq 0.9Hz \quad (14)$$

Also, the simulation result shows  $\Delta f_{max} = 0.91Hz$  (Fig. 12 (a)), which is very close to the obtained value in (14). Also, as expected, the active power of the equivalent unit increases in a ramp manner and are limited to  $R_{max-eq}$  (Fig. 12 (b)).

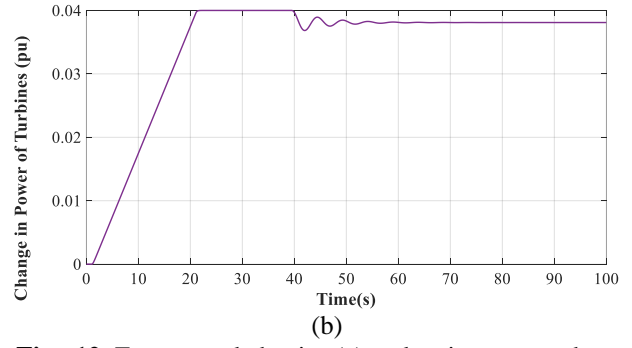
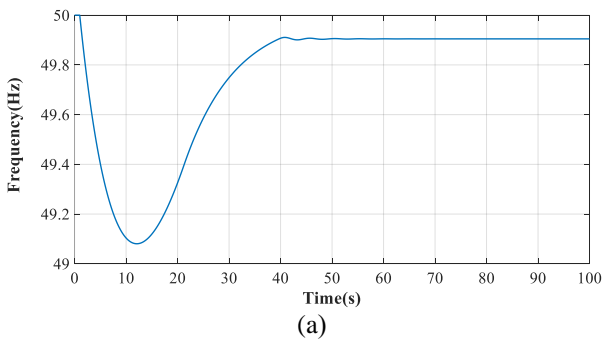


**Fig. 12.** Frequency behavior (a) and active power change (b) in the grid, after  $\Delta P_L = 0.04 pu$  for defined PFR

- B.** Also, for a disturbance  $\Delta P_L = 0.04 pu$ , the PFR volume as  $P_{max-eq} = 0.02 pu$ ,  $R_{max-eq} = 0.002 pu/s$ , and the system parameters presented in Table 3, the value of  $\Delta f_{max}$  from (13) will be as follows.

$$\Delta f_{max} = \max(0.02, 0.018) \triangleq 1Hz \quad (15)$$

Also, the simulation result of the system shows  $\Delta f_{max} = 1Hz$  (Fig. 13 (a)), which is compatible with the obtained answer in (15). It can be seen from Fig. 13 (b) that the active power of the equivalent unit increases in a ramp manner limited to  $R_{max}$ , and before the reaching of frequency to  $f_{min}$ , all PFR is released.

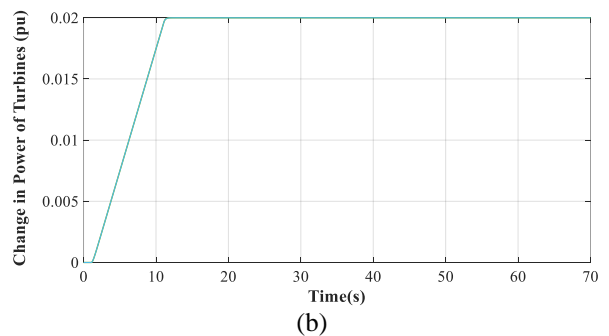
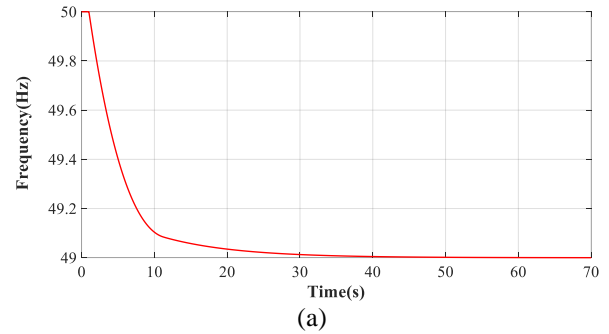


**Fig. 13.** Frequency behavior (a) and active power change (b) in grid, after  $\Delta P_L = 0.04 pu$  for defined PFR.

## 6. Proposed Plan for the Allocation of PFR

As noted earlier, to establish the N-1 security criterion in the grid, PFC should be able to prevent frequency drop to  $f_{sh-1}$  after the trip of the largest generation unit. Accordingly, with the help of the equation provided for  $\Delta f_{max}$  in (13), the minimum requirement for PFR, including its amount, speed, and its allocation strategy can be determined.

$$f_{1-shed} + 0.1 < 50 - \frac{\Delta P_L^{max} \cdot D_{eq} + 2H_{eq} R_{max-eq} \ln \left( \frac{2H_{eq} R_{max-eq}}{2H_{eq} R_{max-eq} + \Delta P_{Lpu} \cdot D_{eq}} \right)}{D_{eq}^2} \quad (17)$$

6.1 PFR volume

Similar to the previous standards [10], PFR volume is determined based on the generation of the largest unit in the grid. While the effect of the parameter  $D_{eq}$  should be considered. Indeed, in the large power systems, the effect of  $D_{eq}$  is considerable, and its corresponding load reduction can alleviate the amount of required PFR. According to the largest single outage ( $\Delta P_L^{max}$ ) and the effect of  $D_{eq}$  on load reduction, the following relation can be used to determine the amount of PFR [7].

$$PFR = \Delta P_L^{max} - D_{eq} (50 - f_1) \tag{16}$$

Where  $f_1$ , is the minimum acceptable frequency of the grid after  $\Delta P_L^{max}$ . It should be noted that all terms in (16) are in per unit in the same power base. Besides, for a given power grid with a definite  $\Delta P_L^{max}$ , the value of  $D_{eq}$  is not constant and depends on the grid load level and their types. In other words, by decreasing the network load, the per-unit value of  $D_{eq}$  is reduced, and in turn, more amount of reserve is needed.

6.2 PFR Speed

Given the first frequency threshold of UFLS ( $f_{1-shed}$ ), the PFR speed ( $R_{max-eq}$ ) should be such that, based on (12), the inequality of (17) is satisfied.

The value of 0.1 on the left side of (17) is considered as a confidence level for sure prevention of UFLS in  $\Delta P_L^{max}$  occurrence. Indeed, the PFR is determined in such a way that with the trip of the largest unit, the frequency nadir is at least 0.1 Hz higher than  $f_{1-shed}$ .

Solving (17) for  $R_{max-eq}$  is not easy. Instead, the right-hand side of the inequality can be depicted for different values of  $R_{max-eq}$ , and considering  $f_{1-shed}$ , the minimum required of the reserve speed is determined. For example, for a system with the parameters presented in Table 3, the value of  $f_{min}$ , for different values of  $R_{max-eq}$ , is shown in Fig 14. It can be seen that the minimum value of the required  $R_{max-eq}$  for  $f_{1-shed} = 49.4 \text{ Hz}$  is 0.0094 pu/s.

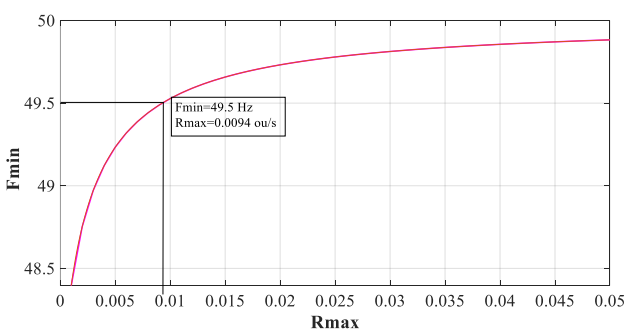


Fig. 14. Frequency nadir for different values of the reserve speed.

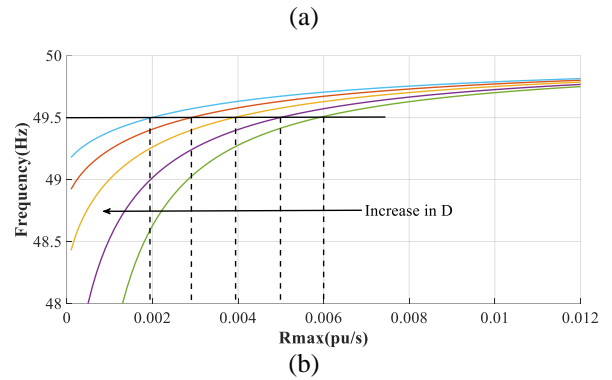
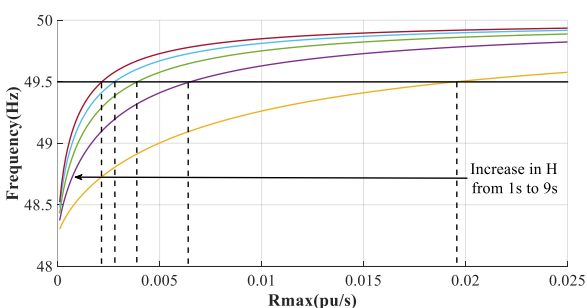


Fig. 15. Frequency nadir, (a) for different values of reserve speed and  $D_{eq}$ , (b) for different values of reserve speed and  $H_{eq}$

Based on (17), the required speed for PFR depends on the  $H_{eq}$  and  $D_{eq}$ . In this regard, the value of  $f_{min}$ , for different value of  $R_{max-eq}$ ,  $H_{eq}$ , and  $D_{eq}$  is shown in Fig 15. It can be seen from Fig. 15 (a) that the decrease in the value of  $D_{eq}$ , from 2 to 0.1, considerably increases the required PFR speed from about 0.002pu/s to 0.006pu/s. Also, decrease of  $H_{eq}$  from 9s to 1s considerably increases the required PFR speed from about 0.002pu/s to 0.02pu/s (Fig. 15 (b)). In fact, by decreasing the values of  $H_{eq}$  and  $D_{eq}$ , according to (10) and (11), the value of  $t_{min}$  decreases, and the primary control has less time to compensate power imbalance.

Considering  $R_{max-eq} = \sum R_{max-i}$ , in order to get the higher speed of PFR, more units should participate in the PFC; while, in small networks, due to the constraints on the number of units, the speed of reserve is limited intrinsically. Therefore, the capacity of the largest generation unit cannot be higher than a special value. Also, for a larger grid with a definite  $\Delta P_L^{max}$ , the value of  $D_{eq}$  and  $H_{eq}$  decrease in low load conditions, and whereby, more speed of PFR is required, and a greater number of units should be used in PFC.

6.3 Proposed PFR allocation plan

Based on the analyses and studies carried out in the previous sections, the following recommendations are proposed to allocate a proper PFR. The proposed scheme is depicted in the flowchart of Fig. 16.

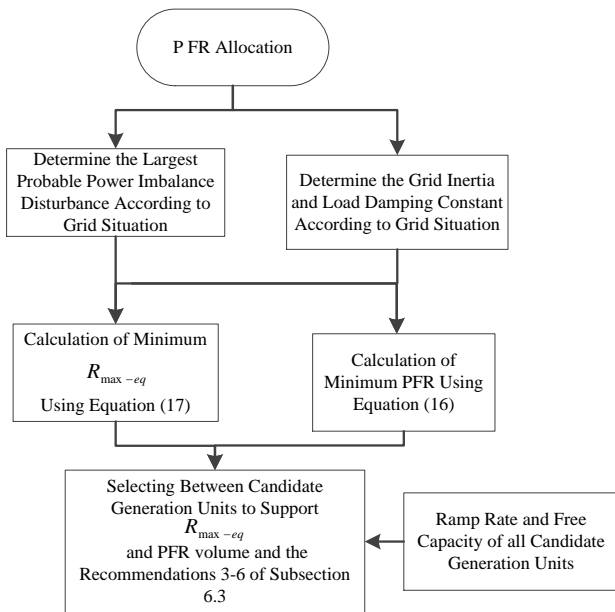


**Fig. 16.** Overall flowchart of the proposed PFR allocation scheme.

1. The PFR volume must be greater than or equal to the value obtained from equation (16).

2. The average reserve speed ( $R_{max-eq} = \Delta P_{m-eq}(t_{min}) / t_{min}$ ) must be greater than or equal to the value obtained from equation (17).

3- In allocating the reserve between the units, the SFR model, was shown in Fig. 2, should be considered as the base model. Then, selection of units for participating in PFC, and the allocation of reserve between them should be such that the  $P_{max-eq} = \sum P_{max-i}$  be more than the value obtained in clause 1 and the requirement of clause 2 should be met. To achieve this, in addition to the use of high-speed units, a greater number of units should be considered for PFC.

4. In order to establish the conditions of clause 3 with a minimum number of units (which leads to less operating costs), the total PFR should be divided equally between units. It means that, at least, for  $t < t_{min}$ ,  $P_m$  of no unit should reach its  $P_{max}$ . It is noted that, if, before  $t_{min}$ ,  $P_m$  of some units reaches to their  $P_{max}$ , the average reserve speed ( $R_{max-eq} = \Delta P_{m-eq}(t_{min}) / t_{min}$ ) becomes less than  $\sum R_{max-i}$ , which may result in  $f_{min} < f_{1-shed}$  and activation of UFLS.

5. According to the results of Section 4, to prevent the increase of  $R_{eq}$  which results in more  $\Delta f_{\infty}$ , the PFR should be distributed between units proportional to their nominal power (the units with the higher nominal power should provide more PFR). Otherwise,  $\Delta f_{\infty}$  will be high, which is a negative point in the operation of a grid.

6. In the low load level of the grid, the value of  $H_{eq}$  and  $D_{eq}$  decreases, and as a result, the grid needs a faster PFR. In this case, considering that the number of synchronized units is low, it's harder to meet the above-mentioned conditions for the PFR. Hence, in PFR allocation, the main attention of grid operators should be paid to low load conditions. Also, in small scale grids, the capacity of the largest generation unit should not be very high; otherwise, the operator will have many difficulties in allocating the PFR, and the PFR cost increases significantly.

## 7. Conclusion

In this paper, the effect of grid dynamic characteristics, including inertia constant, load damping constant, speed and volume of PFR, and the mechanism of distributing PFR between units on the frequency behavior of the grid was investigated. Based on the investigation results, an optimal scheme for allocating PFR (in the form of some equations, instructions, and flowchart) was presented. The proposed scheme considers all effective parameters; hence, it is not needed to have a conservative PFR allocation scheme. Indeed, with a minimum volume of reserve and correct distribution of PFR between the candidate unit, the cost of PFR was reduced. The proposed scheme is not only applicable for large traditional power systems, but it can also be used for microgrids with non-zero inertia. Furthermore, the proposed scheme can be used in the grid restoration process and the design of under frequency load shedding schemes.

## REFERENCES

- [1] J. Machowski, J. W. Bialek, and J. R. Bumby, *Power System Dynamics. Stability and Control*, 2012.
- [2] "IEEE Guide for Abnormal Frequency Protection for Power Generating Plants," *IEEE Std C37.106-2003 (Revision of ANSI/IEEE C37.106-1987)*, pp. 0\_1-34, 2004.
- [3] L. Saarinen, P. Norrlund, W. Yang, and U. Lundin, "Allocation of Frequency Control Reserves and Its Impact on Wear and Tear on a Hydropower Fleet," *IEEE Transactions on Power Systems*, vol. 33, pp. 430-439, 2018.
- [4] J. J. Ford, H. Bevrani, and G. Ledwich, "Adaptive load shedding and regional protection," *International Journal of Electrical Power & Energy Systems*, vol. 31, pp. 611-618, 2009.
- [5] M. Rouholamini, S. E. Jafarabadi, "Simultaneous Scheduling of Energy and Frequency Control Ancillary Services in regard to Load Self-regulation Effect," *TABRIZ JOURNAL OF ELECTRICAL ENGINEERING*, vol. 46, pp. 197-207, 2016 (in persian).
- [6] Y. Rebours and D. s. Kirschen, "What is spinning reserve?", *The University of Manchester*, 2005.
- [7] L. R. Chang-Chien, Y. J. Lin, and C. C. Wu, "An Online Approach to Allocate Operating Reserve for an Isolated Power System," *IEEE Transactions on Power Systems*, vol. 22, pp. 1314-1321, 2007.
- [8] Y. Rebours and D. s. Kirschen, *A Survey of Definitions and Specifications of Reserve Services* vol. releas 1: University of Manchester, 2005.
- [9] F. D. Galiana, F. Bouffard, J. M. Arroyo, and J. F. Restrepo, "Scheduling and Pricing of Coupled Energy and Primary, Secondary, and Tertiary Reserves," *Proceedings of the IEEE*, vol. 93, pp. 1970-1983, 2005.
- [10] Z. Jlassi, K. B. Kilani, M. Elleuch, and C. Bouchoucha, "Primary reserves management in power systems," *13th International Multi-Conference on Systems, Signals & Devices (SSD)*, pp. 194-199, 2016.
- [11] M. A. Bucher, M. A. Ortega-Vazquez, D. S. Kirschen, and G. Andersson, "Robust allocation of reserves considering different reserve types and the flexibility from HVDC," *IET Generation, Transmission & Distribution*, vol. 11, pp. 1472-1478, 2017.

- [12] J. Schipper, A. Wood, and C. Edwards, "Optimizing Instantaneous and Ramping Reserves With Different Response Speeds for Contingencies—Part I: Methodology," *IEEE Transactions on Power Systems*, vol. 35, pp. 3953-3960, 2020.
- [13] Y. Yang, C. Shen, C. Wu, and C. Lu, "Control Performance Based Dynamic Regulation Reserve Allocation for Renewable Integrations," *IEEE Transactions on Sustainable Energy*, vol. 10, pp. 1271-1279, 2019.
- [14] J. Wang, J. Su, Y. Zhao, X. Pang, J. Li, and Z. Bi, "Performance assessment of primary frequency control responses for thermal power generation units using system identification techniques," *International Journal of Electrical Power & Energy Systems*, vol. 100, pp. 81-90, 2018.
- [15] W. Yang, J. Yang, W. Guo, and P. Norrlund, "Response time for primary frequency control of hydroelectric generating unit," *International Journal of Electrical Power & Energy Systems*, vol. 74, pp. 16-24, 2016.
- [16] D. Chakravorty, B. Chaudhuri, and S. Y. R. Hui, "Rapid Frequency Response From Smart Loads in Great Britain Power System," *IEEE Transactions on Smart Grid*, vol. 8, pp. 2160-2169, 2017.
- [17] M. Ramezanzade; M. Jafari-Nokandi; T. Barforoshi, "Scheduling of Generation and Reserve of Thermal Generation Resources Considering Load and Wind Uncertainty in Presence of Energy Storage and Demand Response," *TABRIZ JOURNAL OF ELECTRICAL ENGINEERING*, vol. 48, 2018 (in persian).
- [18] G. Zhang, E. Ela, and Q. Wang, "Market Scheduling and Pricing for Primary and Secondary Frequency Reserve," *IEEE Transactions on Power Systems*, vol. 34, pp. 2914-2924, 2019.
- [19] F. Chengwei, W. Xiaoru, T. Yufei, and W. Wencheng, "Minimum frequency estimation of power system considering governor deadbands," *IET Generation, Transmission & Distribution*, vol. 11, pp. 3814-3822, 2017.
- [20] I. Egido, F. Fernandez-Bernal, P. Centeno, and L. Rouco, "Maximum Frequency Deviation Calculation in Small Isolated Power Systems," *IEEE Transactions on Power Systems*, vol. 24, pp. 1731-1738, 2009.
- [21] L. Liu, W. Li, Y. Ba, J. Shen, C. Jin, and K. Wen, "An Analytical Model for Frequency Nadir Prediction Following a Major Disturbance," *IEEE Transactions on Power Systems*, vol. 35, pp. 2527-2536, 2020.
- [22] H. Li, C. Li, and Y. Liu, "Maximum frequency deviation assessment with clustering based on metric learning," *International Journal of Electrical Power & Energy Systems*, vol. 120, p. 105980, 2020.
- [23] D. Zografos, T. Rabuzin, M. Ghandhari, and R. Eriksson, "Prediction of Frequency Nadir by Employing a Neural Network Approach," *IEEE PES Innovative Smart Grid Technologies Conference Europe (ISGT-Europe)*, pp. 1-6, 2018.
- [24] P. M. Anderson and A. A. Fouad, *Power System Control and Stability, 2ND ED*: Wiley India Pvt. Limited, 2008.
- [25] R. Spangler and R. Shoultz, "Power Generation, Operation, and Control [Book Review]," *IEEE Power and Energy Magazine*, vol. 12, pp. 90-93, 2014.
- [26] P. Kundur, J. Paserba, V. Ajjarapu, G. Andersson, A. Bose, C. Canizares, *et al.*, "Definition and classification of power system stability IEEE/CIGRE joint task force on stability terms and definitions," *IEEE Transactions on Power Systems*, vol. 19, pp. 1387-1401, 2004.